East European Journal of Physics. **2.** 279-282 (2024)
DOI:10.26565/2312-4334-2024-2-29 ISSN 2312-4334

MECHANISM OF CHANGE IN THE EMISSION AND OPTICAL PROPERTIES OF W AND Mo AFTER BOMBARDMENT WITH LOW-ENERGY IONS

D.A. Tashmukhamedova[a]*, B.E. Umirzakov[a], Y.S. Ergashov[b], F.Y. Khudaykulov[c], X.E. Abdiev[a]
[a]*Tashkent State Technical University named after Islam Karimov, Tashkent, 100095 Republic of Uzbekistan*
[b]*National University of Uzbekistan named after Mirzo-Ulugbek, Tashkent, 100173 Republic of Uzbekistan*
[c]*Belarusian-Uzbek Intersectoral Institute of Applied Technical Qualifications in Tashkent, 100071 Republic of Uzbekistan*
**Corresponding Author e-mail: abdiev.xasan.92@bk.ru*
Received February 21, 2024; revised March 28, 2024; accepted April 2, 2024

The paper reports the results of study of composition, emission, and optical properties of polycrystalline W and Mo samples implanted with Ba^+ ions and coated with submonolayer Ba atoms by applying Auger electron spectroscopy, secondary electron emission coefficient σ technique, as well as the photoelectron quantum yield Y. The experimental part was carried out by using the instrumentation and under vacuum P ≈ 10^{-6} Pa. It is shown that during the implantation of Ba ions in the surface layers of refractory metals, a mechanical mixture of the W + Ba and Mo-Ba types is formed. It has been established that the values of the coefficient of secondary electron emission σ and the quantum yield of photoelectrons Y at the same value of the work function eφ in the case of implantation of Ba^+ ions are much larger than in the case of deposition of atoms. The obtained experimental results are substantiated by theoretical calculations.
Keywords: *Mechanical bonds; Ion implantation; Emission efficiency; Auger spectrum; Quantum yield; Plasma oscillations; Fermi level*
PACS: 61.72.uj, 68.55.Ln

INTRODUCTION

Over recently, refractory metals, in particular Mo, W and their alloys, have been widely used and could also be used in the aviation and rocket building industries, i.e., in the development of new generation high-performance gas-tube engines [1-4], thus improving the resistance to plasma beams of the first wall of thermonuclear reactors [5-6], as well as in vacuum technologies and microwave devices [7,8].

Under the influence of ions and plasma on the material, the material is sputtered and evaporated, the structure and phase state change, new chemical compounds are formed on the surface, etc. [9]. At the same time, it is very important to minimize the erosion of materials both during normal functioning and transient events alike, as well as the appropriate choice of these materials is essential [10]. On this purposes, W and Mo can be used, which are characterized by a set of unique physical properties: low physical sputtering ratio, high melting point, high thermal conductivity, low accumulation of tritium. After exposure to plasma irradiation, the creation of an etching relief on the surfaces of metals and alloys is determined by tracing ionic component. Also, the nature of erosion of materials significantly depends on the operating temperature range. The results of [1] show that when tungsten and molybdenum are irradiated with hydrogen plasma, the main relief-forming mechanism happens to be surface sputtering, which is characterized by thermal etching of the surface. In this case, the development of the relief on the tungsten surface due to different erosion rates of adjacent areas during plasma irradiation is due to the fact that differently oriented surface crystals are characterized by different sputtering coefficients [11]. It was found that after irradiation, a fragmented substructure is observed in the surface layer of molybdenum.

At present, the physical and chemical properties of such structures obtained by sputtering, thermal diffusion, and mixing of fine particles with subsequent pressing are well studied. One of the promising methods for engineering a nanofilm structure in the surface layer of materials of various nature is the method of low-energy ion implantation in combination with annealing [12–14]. The use of materials with surface nanosized structures in a particular area of electronic technology is mainly determined by the composition and structure of the surface [15–18].

The present research is devoted to studying the effect of ion implantation on the composition, emission, and optical properties of polycrystalline samples of W and Mo.

EXPERIMENTAL TECHNIQUE

Mo(111) and W(111) single-crystal wafers with a diameter of 8 – 10 mm and a thickness of 0.8 mm were used for experiments. Ion implantation, annealing and all studies using Auger electron spectroscopy (AES), measurements of the total secondary electron emission (SEE) coefficient σ and photoelectron quantum yield Y were carried out by using the same experimental instrumentation under ultrahigh vacuum conditions (P = 10^{-6} Pa). Ba^+ ions were obtained by surface ionization of Ba atoms. The diameter of the ion beam on the sample surface was ~ 1.5…2 mm. Implantation with Ba^+

Cite as: D.A. Tashmukhamedova, B.E. Umirzakov, Y.S. Ergashov, F.Y. Khudaykulov, X.E. Abdiev, East Eur. J. Phys. 2, 279 (2024), https://doi.org/10.26565/2312-4334-2024-2-29

ions was carried out mainly with energy E_0 = 1 keV and dose D = $6 \cdot 10^{16}$ cm^{-2} (saturation dose). The current of Ba^+ ions could be increased up to ~0.3 μA. The experimental technique is described in more detail in [18].

EXPERIMENTAL RESULTS AND DISCUSSION

On Fig. 1 shows the dependences σ(E_p) for pure W and W implanted with Ba^+ ions with energy E_0=0.5 keV at a dose of D = $6 \cdot 10^{16}$ cm^{-2} and coated with Ba atoms ~ 1 monolayer thick. On Fig. 2 for the same samples shows the dependences of the photoelectron quantum yield Y on the photon energy in the range hν = 2 – 6 eV.

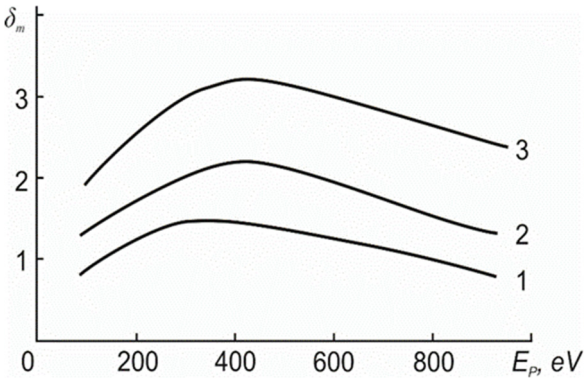

Figure 1. Dependences σ$_m$(Ep) for: 1 – W(111), 2 – W(111) with surface film Ba with θ ≈ 1 monolayer, 3 – W implanted with Ba^+ ions with E = 0.5 keV at D = $6 \cdot 10^{16}$ cm^{-2}

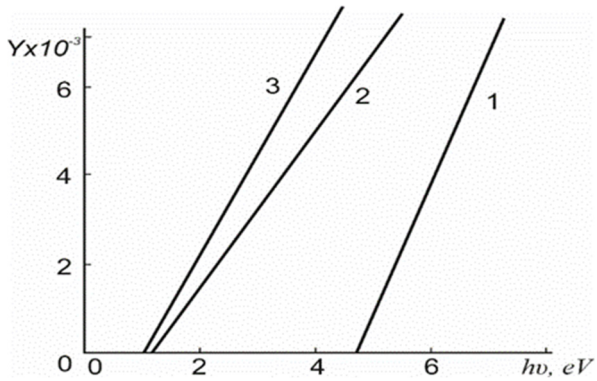

Figure 2. Dependences of Y½ on hν for: 1 – pure W(111), 2 - W(111) with a Ba film with a thickness of 1 monolayer, 3 - W(111) implanted with Ba^+ ions with E = 0.5 keV at D = $6 \cdot 10^{16}$ cm^{-2}

To determine the concentration and mobility of charge carriers at the base region of the structure, the authors have applied the Hall factor technique at various temperatures. Also the authors have studied the photovolt-ampere characteristic at various values of monochromatic illumination at ($h\nu \geq E_g$).

It can be seen from these figures that the increase in σ and Y of tungsten in the case of implantation of Ba^+ ions is significantly greater than in the case of deposition of Ba with a thickness of θ ≈ 1 monolayer.

It is known that the increase in the SEE coefficient σ and the quantum yield of photoelectrons in the case of deposition (at θ ≃ 1) is mainly determined by a decrease in the work function, and in the case of ion doping, both by a decrease in eφ and by a change in the bulk physical properties of the emitting layer [19, 20].

The true secondary electrons (TSE) coefficient δ can be determined by the following formula:

$$\delta = \int_0^\infty n(E_P, x) \cdot f(x) \cdot dx, \quad (1)$$

where $n(Ep, x)$ is the density of internal secondary electrons formed primary electrons with energy Ep at depth x; $f(x)$ – probabilities exit of secondary electrons from this depth x. $f(x)$ is defined as

$$f(x) = \psi(x) \cdot p(e\varphi), \quad (2)$$

where $\psi(x)$ is the probability that electrons from depth x will approach the surface, and $p(e\varphi)$ is the probability of exit of secondary electrons approaching the metal-vacuum boundary. Thus, δ depends both on the work function and on the density of internal secondary electrons n(E_p, x) formed by primary electrons in the IVE exit zone – λ.

In order to evaluate the role of the surface and volume in increasing the coefficients σ$_m$ and Y of ion-doped samples, we compared the results of measurements of Y and σ$_m$ for W coated with a barium layer of different thicknesses and doped with Ba^+ ions with different energies at D=D$_{sat}$=$6 \cdot 10^{16}$ см$^{-2}$ (D$_{sat}$ - saturation dose). For comparison, such values of the ion energy E_o and layer thickness θ were chosen at which the work function for both samples was approximately the same (Table 1).

Table 1. Values of σ_m, Y and eφ for W(111) implanted with barium ions with different energies and coated with a barium layer of different thicknesses

$Ba^+ \rightarrow$ W, D = $6 \cdot 10^{16}$ см$^{-2}$				Ba/W				σ_i/σ_d	Y_i/Y_d
E_0, keV	σ_m	Y·10^6	eφ	θ	σ_m	Y·10^6	eφ		
0.5	3.4	56	2.3	0.7	2.0	30	2.35	1.7	1.8
3.0	2.6	30	3.2	0.4	1.75	19	3.15	1.45	1.6
5.0	2.1	11	3.9	0.2	1.55	9	3.85	1.3	1.2

The values $\sigma = \sigma_m$ corresponded to the energy E_{pm} ≈ 450 – 500 eV.

It can be seen from the table that, with the same changes in eφ, the values σ_m of σm and Y for doped samples are greater than for deposited ones. A significant difference in σ and Y between implanted and deposited samples is observed at E_0 = 1 keV, and in this case σ_i/σ_d and Y_i/Y_d are ~ 1.7. The calculated value of the depth of the EVE and photoelectron exit zone for pure W was 20 – 25 Å.

In this case, the main part of the intercalated atoms is located at a depth of 0 – 20 Å, which is close to the ISE exit zone. This, as well as a strong decrease in eφ, explains the largest increase in σ and Y at E_0 = 0.5 – 1 keV. As the ion energy increases, the concentration of interstitial atoms in the emitting layer decreases, which leads to a decrease in the ratio σ_l/σ_n and Y_l/Y_n.

According to formula (1), the growth of σ and Y in the case of doping is associated with an increase in the density of internal secondary electrons $n(Ep, x)$, which is proportional to the energy loss per unit path of the primary or inelastically reflected electron:

$$dE/dx = n_e \int_0^\infty \varepsilon \cdot d\delta(E, \varepsilon). \quad (3)$$

Here (E, ε) is the differential scattering cross section with energy loss ε. The value of ne increases significantly with increasing impurity concentration in the emitting layer.

At low energies of primary electrons, a certain contribution to the number of TSEs and photoelectrons comes from those electrons of the introduced impurity that are located at the upper energy levels. Table 2 lists the energies of the levels of Mo, W, and Ba atoms.

Table 2. Energy levels of Mo, W, and Ba atoms

Mo	N_{45}	N_{23}	N_1	M_5	M_4	M_3	M_2
	2	35	62	227	230	392	410
W	P_1	N_7	N_6	N_5	N_4	N_3	N_2
	4	34	37	46	259	426	492
Ba	V	O_3	O_2	O_1	N_5	N_4	N_3
	3	15	17	39	90	92	180

It can be seen that many of the barium levels are located in the band gap region of Mo, W. For example, the Ba levels with energies of 3, 15, 17 eV are located between the conduction band and the first filled Mo band. The probabilities of excitation of electrons from these levels Ba are greater than the probabilities of excitation of electrons from the filled Mo band (in addition, the ionization of O_3 and O_2 levels can lead to the appearance of the O_2VV and O_3VV Auger process). Therefore, in the region of small E_p at high impurity concentrations, these levels will make a significant contribution to the number of TSEs, the presence of such levels also increases the inelastic reflected electrons (IRE) efficiency.

In the case of metals W and Mo, the formula [21] can also be used for calculation

$$\delta = \frac{B}{\varepsilon} \int_0^\infty F(x) e^{-\frac{\lambda}{x}} dx. \quad (4)$$

Here F(x) is the energy loss distribution function of absorbed and inelastically reflected electrons. B is the probability of exit of SEs approaching the surface, and ε is the average energy required for the formation of one secondary or photoelectrons, λ is the depth of exit of the EVE. The values of λ range from 10 to 30 Å for most metals, and the value $\frac{\varepsilon}{B}$, according to Dekker, does not depend on the energy of primary electrons and has a value of ~ 100 ÷ 200. We performed calculations for λ = 10, 15, 20 and 30 Å. The best agreement with experiment is obtained in the case of λ =10 Å: ε/B = 140 for Mo and 170 for W.

Table 3 shows the calculated δ_C and experimental δ_E values of the TSE coefficients for Mo and W. It can be seen from the table that agreement with experiment is good for E_p > 800 eV, and for lower E_p, the calculated values turn out to be lower than the experimental ones.

The reason is that at such energies the parameter ε/B begins to depend on the energy of the primary electron.

Table 3. Calculated and experimental values of true-secondary electron coefficient δ_m

	E_0, эВ	600	800	1000	3000	4000
Mo	δ_C	0.87	0.95	0.94	0.54	0.45
	δ_E	0.98	0.95	0.92	0.55	0.46
W	δ_C	0.7	0.78	0.84	0.56	0.46
	δ_E	0.91	0.88	0.81	0.6	0.48

Indeed, at low energies, the role of excitation and decay of plasmons in the formation of SE increases and the mechanism of excitation of electrons from deep levels is "switched off", which should lead to a decrease in ξ - the average energy spent on the formation of one SE. At the same time, the conditions for the release of secondary electrons also change. The results obtained are consistent with the conclusions that, at large E_0, the SEE coefficients are determined mainly by the energy losses of primary electrons, but not by the secondary electron release mechanism.

CONCLUSIONS

It is shown that the increase in the coefficient of secondary electron emission and the quantum yield of W and Mo photoelectrons after implantation of Ba^+ ions is mainly due to a decrease in the work function of the surface and an increase in energy losses for the absorption of electrons in the ion-implanted layer.

It has been found that at low electron energies ($E \leq 0.8$ keV), the calculated values of the TSE coefficient are significantly lower than the experimental ones. For $E_0 \geq 1$ keV, they are in good agreement with each other.

The results obtained are employed in various branches of electronic and chemical industry, in particular, production of pure Mo and its alloys and catalysts for processing of oil and oil products and are promising in the development of OLED displays, optical resonators and filters, sensors, and solar cells.

ORCID

D.A. Tashmukhamedova, https://orcid.org/0000-0001-5813-7518; **B.E. Umirzakov,** https://orcid.org/0000-0002-9815-2111
Y.S. Ergashov, https://orcid.org/0000-0002-1884-9462; **F.Y. Khudaykulov,** https://orcid.org/0009-0000-7250-3836
X.E. Abdiev, https://orcid.org/0000-0003-3843-1503

REFERENCES

[1] B.K. Rakhadilov, A.Zh. Miniyazov, M.K. Skakov, Zh.B. Sagdoldina, T.R.Tulenbergenov, and E.E. Sapataev, Technical Physics, **65**, 382 (2020). https://doi.org/10.1134/S1063784220030202
[2] V. Kurnaev, I. Vizgalov, K. Gutorov, T. Tulenbergenov, I. Sokolov, A. Kolodeshnikov, and V. Ignashev, J. Nucl. Mater. **463**, 228 (2015). https://doi.org/10.1016/j.jnucmat.2014.12.076
[3] J. Roth, E. Tsirone, A. Loarte, Th. Loarer, G. Counsell, R. Neu, V. Philipps, et al., J. Nucl. Mater. **390–391**, 1 (2009). https://doi.org/10.1016/j.jnucmat.2009.01.037
[4] T. Teusch, and T. Kluener, Journal of Physical Chemistry C, **123** (46), 28233 (2019). https://doi.org/10.1021/acs.jpcc.9b08268
[5] O.G. Ospennikova, V.N. Pod'yachev, and Yu.V. Stolyankov, Trudy VIAM, 10(46), 55 (2016). https://doi.org/10.18577/2307-6046-2016-0-10-5-5 (in Russian)
[6] E.N. Kablov, Aviation materials and technologies, **1**(34), 3 (2015). https://doi.org/10.18577/20719140-2015-0-1-3-33 (in Russian)
[7] Y. Yao, D. Sang, L. Zou, Q. Wang, and C. Liu, Nano-materials, **11**(8), 2136 (2021). https://doi.org/10.3390/nano11082136
[8] E.P. Surovoi, V.E. Surovaia, and L.N. Bugerko, J. Phys. Chem. A, **87** (5), 826 (2013). https://doi.org/10.1134/S0036024413050257
[9] ITER Joint Central Team, Report No. G AO FDR 4 01-07-21 R0.4 (Garching, 2001).
[10] V. Philipps, J. Roth, and A. Loarte, Plasma Phys. Control. Fusion, **45**, A17 (2003). https://doi.org/10.1088/0741-3335/45/12A/002
[11] B.K. Rakhadilov, M.K. Skakov, and T.R. Tulenbergenov, Key Engineer. Mater. **736**, 46 (2017). https://doi.org/10.4028/www.scientific.net/KEM.736.46
[12] E.S. Ergashov, D.A. Tashmukhamedova, and B.E. Umirzakov, Journal of Surface Investigation: X-ray, Synchrotron and Neutron Techniques, **11**, 480 (2017). https://doi.org/10.1134/S1027451017020252
[13] D.A. Tashmukhamedova, and M.B. Yusupjanova, Journal of Surface Investigation: X-ray, Synchrotron and Neutron Tech. **10**(6), 1273 (2016). https://doi.org/10.1134/S1027451016050438
[14] B.E. Umirzakov, D.A. Tashmukhamedova, and F.Ya. Khudaykulov, Journal of Surface Investigation: X-ray, Synchrotron and Neutron Techniques, **16**(6), 992 (2022). https://doi.org/10.1134/S1027451022050202
[15] B.E. Umirzakov, A.K. Tashatov, D.A. Tashmukhamedova, and M.T. Normuradov, Poverkhnost. Rentgenovskie, Sinkhronnye i Nejtronnye Issledovaniya, **12**, 90 (2004). https://www.elibrary.ru/item.asp?id=17669389. (in Russian)
[16] D.A. Tashmukhamedova, B.E. Umirzakov, and M.A. Mirzhalilova, Izvestiya Akademii Nauk. Ser. Fizicheskaya, **68**(3), 424 (2004). https://www.elibrary.ru/item.asp?id=17641066. (in Russian)
[17] D.A. Tashmukhamedova, Izvestiya Akademii Nauk. Ser. Fizicheskaya, **70**(8), 1230 (2006). https://elibrary.ru/item.asp?id=9296378. (in Russian)
[18] D.A. Tashmukhamedova, and M.B. Yusupjanova, Journal of Surface Investigation: X-ray, Synchrotron and Neutron Techniques, **15**(5), 1054 (2021). https://doi.org/10.1134/S1027451021050402
[19] J.B. Biersack, and L.G. Haggmark, Nucl. Instrum. and Meth. **174**(1), 257 (1980). https://doi.org/10.1016/0029-554X(80)90440-1
[20] Y. Yamamura, Y. Mirzuno, and H. Kimura, Nucl. Instr. and Meth. Phys. Res. B, **13**(1-3), 393-395 (1986). https://doi.org/10.1016/0168-583X(86)90535-5
[21] X. Rissel, and I. Ruge, *Ion implantation*, (Nauka, Moscow, 1982). (in Ruassian)

МЕХАНІЗМ ЗМІНИ ЕМІСІЇ ТА ОПТИЧНИХ ВЛАСТИВОСТЕЙ W ТА Mo ПІСЛЯ БОМБАРДУВАННЯ НИЗЬКОЕНЕРГІЙНИМИ ІОНАМИ

Д.А. Ташмухамедова[a], Б.Е. Умірзаков[a], Ю.С. Ергашов[b], Ф.Й. Худайкулов[c], Х.Є. Абдієв[a]

[a]Ташкентський державний технічний університет імені Іслама Карімова, Ташкент, 100095 Республіка Узбекистан
[b]Національний університет Узбекистану імені Мірзо-Улугбека, Ташкент, 100173 Республіка Узбекистан
[c]Білорусько-Узбецький міжгалузевий інститут прикладної технічної кваліфікації, Ташкент, 100071 Республіка Узбекистан

У статті наведено результати дослідження складу, емісійних і оптичних властивостей полікристалічних зразків W і Mo, імплантованих іонами Ba^+ і покритих субмоношаровими атомами Ba, за допомогою Оже-електронної спектроскопії, методу вторинної емісії σ, а також фотоелектронного квантового виходу Y. Експериментальна частина виконувалася апаратурно під вакуумом $P \approx 10^{-6}$ Па. Показано, що під час імплантації іонів Ba у поверхневих шарах тугоплавких металів формується механічна суміш W + Ba та Mo-Ba типу. Встановлено, що значення коефіцієнта вторинної електронної емісії σ та квантового виходу фотоелектронів Y при однаковому значенні роботи виходу eφ у разі імплантації іонів Ba^+ значно більші, ніж у випадку осадження атомів. Отримані експериментальні результати обґрунтовані теоретичними розрахунками.

Ключові слова: *механічні зв'язки; іонна імплантація; ефективність викидів; Оже-спектр; квантовий вихід; плазмові коливання; рівень Фермі*